

# Microwave Spectroscopy of the Twist $C^\beta$ -Exo/ $C^\gamma$ -Endo Conformation of Prolinamide

Kimberly A. Kuhls, Charla A. Centrone, and Michael J. Tubergen\*

Contribution from the Department of Chemistry, Kent State University, Kent, Ohio 44242-0001

Received May 21, 1998

**Abstract:** The rotational transitions of three isotopomers of prolinamide were measured with a Fourier-transform microwave spectrometer. A twist pyrrolidine ring conformation with  $C^\beta$ -exo and  $C^\gamma$ -endo reproduces the experimental moments of inertia. Stark-effect measurements of five  $|M|$  components were used to determine that the dipole moment of this conformation of prolinamide is 3.83(4) D. Kraitchman's method of isotopic substitution was used to determine an N–N distance of 2.684(2) Å.

## Introduction

The conformations of amino acids have been investigated by a variety of experimental and theoretical techniques, including molecular mechanics, NMR spectroscopy, and X-ray crystallography. Structural information about these small biological molecules reveals their conformational preferences and provides insight about the intramolecular forces which stabilize larger peptides and proteins. Conformational studies of gas-phase amino acids are particularly interesting because these conformations can be directly compared with computational models without accounting for the intermolecular effects of condensed media.

Microwave spectra have been recorded for two different conformers of glycine.<sup>1–3</sup> The initial studies<sup>1</sup> compared the experimental rotational constants and dipole moment to values derived from a series of structural models; the reported spectrum was assigned to a conformation containing an intramolecular hydrogen bond from the carboxylic acid to the amino nitrogen. However, Hartree–Fock calculations at the 4-31G level found that another conformer, with hydrogen bonds from the amine to the carbonyl oxygen, is 9.2 kJ mol<sup>-1</sup> more stable than the initially assigned structure.<sup>4</sup> The rotational spectrum of the more stable conformer was later found, but its spectrum was much weaker due to its smaller dipole moment.<sup>2</sup> Lovas and co-workers have recently used a Fourier-transform microwave (FTMW) spectrometer to resolve the hyperfine structure arising from the <sup>14</sup>N nuclear quadrupole moment.<sup>3</sup> The higher resolution also enabled more precise measurements of the Stark shifts of the  $|M_F|$  components and consequently a more accurate determination of the  $\mu_a$  and  $\mu_b$  dipole components.

The microwave spectrum of a second amino acid, alanine, was recorded and assigned to gas-phase conformations similar to those identified for glycine; assignments were again made

by comparison of experimental and theoretical spectra.<sup>5</sup> Nonetheless, microwave spectroscopy of the amino acids has been hampered by low vapor pressures and narrow working temperature ranges. No glycine signal could be observed below 150 °C in the FTMW studies, but temperatures greater than 170 °C caused rapid decomposition.<sup>3</sup>

Among the amino acids, only proline (Figure 1A) has a five-membered-ring system that joins the side chain to the backbone at the amino nitrogen. The five-membered ring restricts torsions about the bond between  $C^\alpha$  and the amino nitrogen, so proline reduces the flexibility of peptides and is often found in the bends and kinks of folded protein chains. Despite proline's unique connectivity, HF/4-21G<sup>6</sup> and HF/6-31G<sup>7</sup> calculations find that the most stable conformation contains an intramolecular hydrogen bond from the amine to the carbonyl oxygen and is similar to the lowest energy glycine and alanine conformers.

The conformations of proline and proline derivatives are complicated by puckering of the pyrrolidine ring, which relieves torsional strain caused by eclipsing methylene groups on the ring edges. Microwave spectra of pyrrolidine<sup>8</sup> (Figure 1B) and *d*<sub>1</sub>-pyrrolidine<sup>9</sup> indicate that the ring adopts an envelope structure with the nitrogen out of plane and the amino hydrogen axial. Electron diffraction experiments and ab initio calculations<sup>10</sup> (HF/4-21 N\*) confirmed that this is the lowest energy conformation and found that the barrier to pseudorotation is 6.95 kJ mol<sup>-1</sup>. *N*-Methylpyrrolidine<sup>11</sup> and *N*-cyanopyrrolidine<sup>12</sup> also have *N*-envelope structures, but with the methyl and cyano groups equatorial.

(5) Godfrey, P. D.; Firth, S.; Hatherley, L. D.; Brown, R. D.; Pierlot, A. P. *J. Am. Chem. Soc.* **1993**, *115*, 9687–9691.

(6) Tarakeshwar, P.; Manogaran, S. *J. Mol. Struct.* **1996**, *365*, 167–181.

(7) Sapse, A.-M.; Mallah-Levy, L.; Daniels, S. B.; Erickson, B. W. *J. Am. Chem. Soc.* **1987**, *109*, 3526–3529.

(8) Caminati, W.; Oberhammer, H.; Pfafferott, G.; Filgueira, R. R.; Gomez, C. H. *J. Mol. Spectrosc.* **1984**, *106*, 217–226.

(9) Ehrlichmann, H.; Grabow, J.-U.; Dreizler, H. Z. *Naturforsch.* **1989**, *44a*, 837–840.

(10) Pfafferott, G.; Oberhammer, H.; Boggs, J. E.; Caminati, W. *J. Am. Chem. Soc.* **1985**, *107*, 2305–2309.

(11) Pfafferott, G.; Oberhammer, H.; Boggs, J. E. *J. Am. Chem. Soc.* **1985**, *107*, 2309–2313. Caminati, W.; Scappini, F. *J. Mol. Spectrosc.* **1986**, *117*, 184–194.

(12) Su, C.-H.; Harmony, M. D. *J. Mol. Spectrosc.* **1985**, *112*, 328–339.

(1) Brown, R. D.; Godfrey, P. D.; Storey, J. W. V.; Bassez, M.-P. *J. Chem. Soc., Chem. Commun.* **1978**, 547–548. Suenram, R. D.; Lovas, F. J. *J. Mol. Spectrosc.* **1978**, *72*, 372–382.

(2) Suenram, R. D.; Lovas, F. J. *J. Am. Chem. Soc.* **1980**, *102*, 7180–7184.

(3) Lovas, F. J.; Kawashima, Y.; Grabow, J.-U.; Suenram, R. D.; Fraser, G. T.; Hirota, E. *Astrophys. J.* **1995**, *455*, L201–L204.

(4) Vishveshwara, S.; Pople, J. A. *J. Am. Chem. Soc.* **1977**, *99*, 2422–2426. Sellers, H. L.; Schäfer, L. *J. Am. Chem. Soc.* **1978**, *100*, 7728–7729. Schäfer, L.; Sellers, H. L.; Lovas, F. J.; Suenram, R. D. *J. Am. Chem. Soc.* **1980**, *102*, 6566–6568.

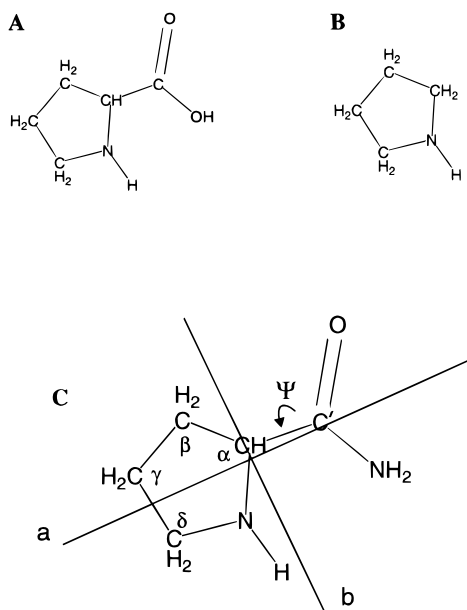


**Figure 1.** Molecular structures of (A) proline, (B) pyrrolidine, and (C) prolinamide. The molecular structure of prolinamide includes the approximate projections of the *a* and *b* inertial axes.  $\Psi$  represents the dihedral angle  $NC^{\alpha}C^{\beta}N$ .

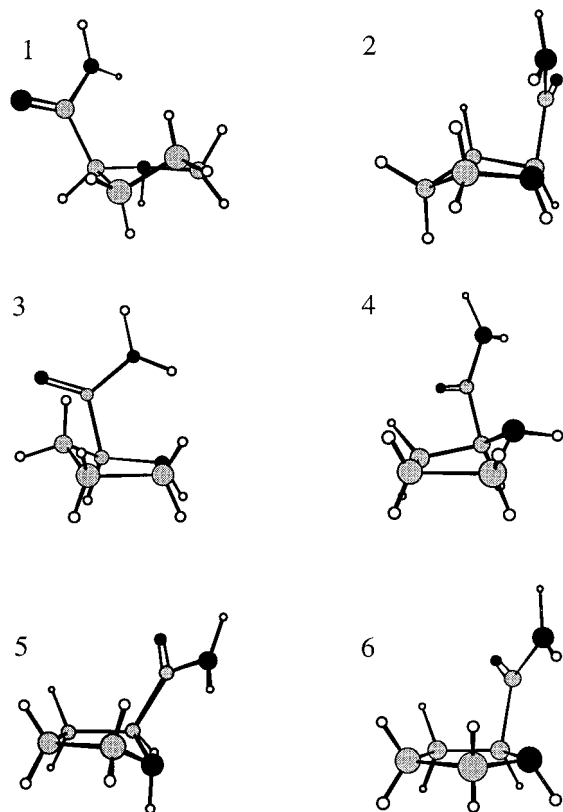


**Figure 2.** Semiempirical model conformers.

Ring puckering in proline and prolinamide may differ from that in pyrrolidine because of the attachment of the carbonyl at  $C^{\alpha}$ ; prolinamide and its principal axes are shown in Figure 1C. The X-ray crystal structure of L-proline,<sup>13</sup> originally interpreted as an envelope conformation, is consistent with a “twist” pyrrolidine ring conformation with  $C^{\beta}$ -exo and  $C^{\gamma}$ -endo<sup>14,15</sup> ( $C^{\beta}$ -

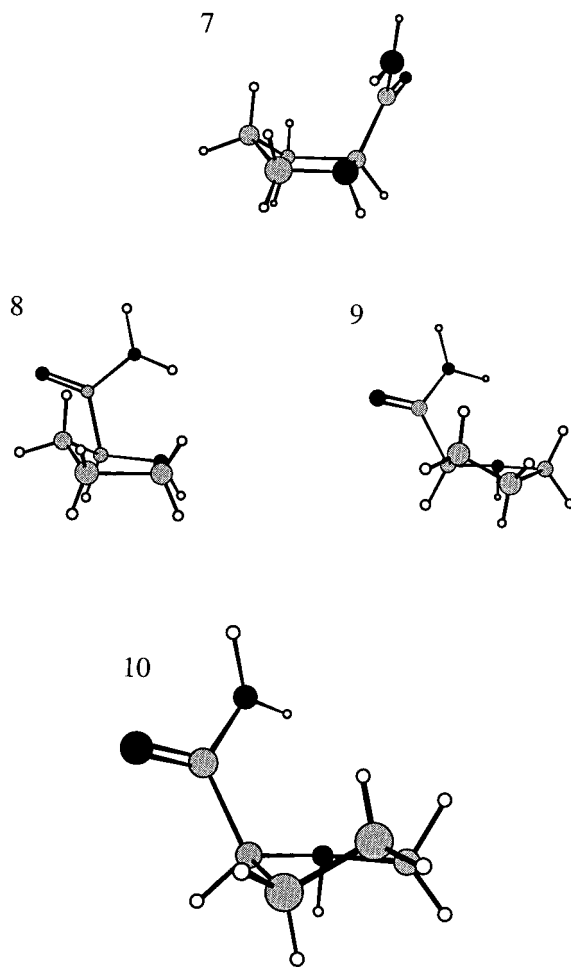


**Figure 3.** Ab initio model conformers. Conformer **10**, which reproduces the experimental data best, is enlarged to show greater detail.

exo indicates that  $C^{\beta}$  and  $C^{\gamma}$  are on the opposite sides of the  $C^{\alpha}$ -N- $C^{\delta}$  plane—see conformer **10** in Figure 3). DeTar and Luthra modeled the ring-puckering conformations of prolyl systems using molecular mechanics and found two broad potential energy minima approximately corresponding to a  $C^{\gamma}$ -exo envelope structure and a  $C^{\beta}$ -exo/ $C^{\gamma}$ -endo twist structure.<sup>14</sup> DeTar and Luthra also investigated proline ring conformations in solution using  $^1H$  and  $^{13}C$  chemical shifts of complexes between *N*-acylproline esters and europium or ytterbium shift reagents; they found that the observed shifts were reproduced by a 60:40 mixture of twist and envelope conformations.<sup>16</sup> Proline ring conformations, determined from the X-ray structures of 40 different proline derivatives and peptides, cluster about these two minima as well.<sup>14</sup>

The ring-puckering conformations of prolyl systems are often described with use of the pseudorotation equation:<sup>15,17</sup>  $\chi_i = \chi_{\max} \cos(P + 4\pi i/5)$  in which  $\chi_i$  represents a bond torsion angle of the ring,  $\chi_{\max}$  is the maximum amplitude of puckering, and  $P$  is the phase angle of puckering. The amplitude and phase of ring puckering have been determined from many X-ray crystallographic and NMR experiments; these experiments indicate that the most frequent conformations have  $P \approx 0^\circ$  or  $P \approx 180^\circ$  and are approximately twist structures with  $C^{\beta}$ -endo and  $C^{\gamma}$ -exo (Haasnoot et al. refer to this as “N-domain”) or the closely

(13) Kayushina, R. L.; Vainshtein, B. K. *Sov. Phys.-Crystallogr.* **1966**, *10*, 698–706.

(14) DeTar, D. F.; Luthra, N. P. *J. Am. Chem. Soc.* **1977**, *99*, 1232–1244.

(15) Haasnoot, C. A. G.; De Leeuw, F. A. A. M.; De Leeuw, H. P. M.; Altona, C. *Biopolymers* **1981**, *20*, 1211–1245.

(16) DeTar, D. F.; Luthra, N. P. *J. Org. Chem.* **1979**, *44*, 3299–3305.

(17) Altona, C.; Sundaralingam, M. *J. Am. Chem. Soc.* **1972**, *94*, 8205–8212.

related  $C^\beta$ -exo/ $C^\gamma$ -endo structure (“S-domain”).<sup>15</sup> The conformational domains are quite broad, however, and include conformations better described as envelopes (including the  $C^\gamma$ -exo envelope structure).

### Experimental Section

The rotational spectra were recorded with a Balle–Flygare<sup>18</sup> spectrometer consisting of a microwave cavity established by two 36-cm diameter aluminum mirrors. The mirrors slide on four 1.27-cm diameter stainless steel rails and can be positioned with a motorized micrometer. Microwave radiation, generated by a Hewlett-Packard 83711B synthesized frequency generator, is coupled into the cavity by an L-shaped antenna; molecular emission is detected by a similar antenna on the opposite mirror and frequency reduced by a heterodyne circuit described elsewhere.<sup>19</sup> The molecular signal is then digitized with use of a Keithley-MetraByte DAS-4101 data acquisition board in a personal computer.

Two solid aluminum plates, 30 cm  $\times$  30 cm  $\times$  0.5 cm, straddle the cavity between the mirrors. The plates are separated by 27 cm and are attached to the mirror guide rails with plastic spacers. Each plate can be charged up to 10 000 V with opposite polarity for Stark effect measurements. The electric field is calibrated by measuring the Stark shift of the 1–0 transition of OCS ( $\mu = 0.715196$  D<sup>20</sup>).

Prolinamide was heated to 150 °C and incorporated into an argon expansion with a backing pressure of 1.5 atm. The expansion was pulsed into the microwave cavity perpendicular to the cavity axis. This arrangement results in Doppler splittings of 25 kHz and a line width of 12 kHz for each component, when measured with carbonyl sulfide. The frequency resolution of the spectrometer, determined by the number of data points recorded for the free induction decay, was 4 kHz for these measurements (1024 data points).

L-Prolinamide was used as purchased from Aldrich. The <sup>15</sup>N-labeled isotopes were prepared by a four-step synthesis starting from L-proline.<sup>21</sup> The first step was to add a carbobenzyloxy protecting group to the proline amino group by reaction with benzyl chloroformate in sodium hydroxide solution. CBZ-proline was obtained as a viscous oil. Next, the carboxylic acid was esterified with *p*-nitrophenol with use of the coupling reagent dicyclohexylcarbodiimide; the needles of CBZ-proline-*p*-nitrophenyl ester melted at 92–94 °C. The amide was formed by reacting the activated ester with anhydrous ammonia generated in a vacuum line from NH<sub>4</sub>Cl and excess NaOH. Subsequent hydrogenation of the CBZ-prolinamide in cyclohexene with palladium catalyst<sup>22</sup> removed the carbobenzyloxy protecting group and resulted in the formation of the desired isotopomer of prolinamide. The final yield of crude product was 40% over the four steps. The intermediate compounds were characterized with use of melting points and FTIR spectroscopy; a sample of <sup>14</sup>N<sub>2</sub>-labeled final product was also characterized by comparison of the rotational spectrum to that of the commercially available material. Two <sup>15</sup>N-labeled isotopomers were synthesized: a single <sup>15</sup>N at the amide position (<sup>15</sup>N<sub>a</sub>-prolinamide), prepared with the most abundant isotope of proline and <sup>15</sup>NH<sub>3</sub>, and the doubly substituted species (<sup>15</sup>N<sub>2</sub>-prolinamide) in which both the amide and amine nitrogens were <sup>15</sup>N labeled. The doubly substituted species was prepared from <sup>15</sup>N-L-proline and <sup>15</sup>NH<sub>3</sub> (Cambridge Isotope Laboratories).

### Results

Twelve *a*- and *b*-type rotational transitions were measured for the most abundant isotope of prolinamide (Table 1). Each rotational transition consists of many hyperfine components arising from the two <sup>14</sup>N nuclei; these components overlap each

**Table 1.** Center Frequencies for the Rotational Transitions of <sup>14</sup>N<sub>2</sub>-Prolinamide

transition	obsd freq, MHz	obsd – calcd, MHz
3 <sub>03</sub> –2 <sub>02</sub>	9025.684	–0.163
3 <sub>13</sub> –2 <sub>12</sub>	8707.280	–0.242
3 <sub>12</sub> –2 <sub>11</sub>	9513.585	–0.072
3 <sub>22</sub> –2 <sub>21</sub>	9126.676	0.034
3 <sub>21</sub> –2 <sub>20</sub>	9227.307	–0.131
4 <sub>04</sub> –3 <sub>03</sub>	11925.940	0.028
4 <sub>14</sub> –3 <sub>13</sub>	11583.590	0.054
4 <sub>13</sub> –3 <sub>12</sub>	12651.430	0.116
2 <sub>12</sub> –1 <sub>01</sub>	7799.835	–0.010
3 <sub>03</sub> –2 <sub>12</sub>	7284.940	0.083
3 <sub>13</sub> –2 <sub>02</sub>	10448.656	0.144
4 <sub>04</sub> –3 <sub>13</sub>	10503.316	0.069

**Table 2.** Spectroscopic Constants for the Isotopic Species of Prolinamide

	prolinamide	<sup>15</sup> N <sub>a</sub> -prolinamide	<sup>15</sup> N <sub>2</sub> -prolinamide
<i>A</i> (MHz)	3640.355 (89)	3593.340 (24)	3558.635 (6)
<i>B</i> (MHz)	1655.717 (20)	1641.516 (7)	1635.443 (3)
<i>C</i> (MHz)	1386.497 (15)	1371.998 (6)	1365.514 (2)
<i>D</i> <sub>J</sub> (kHz)	<i>a</i>	1.1 (2)	0.98 (3)
<i>D</i> <sub>JK</sub> (kHz)	<i>a</i>	–9.5 (11)	–4.2 (1)
<i>d</i> <sub>I</sub> (kHz)	<i>a</i>	<i>a</i>	–0.24 (4)
$\Delta\nu_{\text{rms}}$ (kHz)	114.9	22.4	3.7

<sup>a</sup> Value fixed to 0.0 kHz in the fit.

other and could not be resolved. The rotational transitions, therefore, appeared as broad clusters of partially resolved components spread over 600 kHz. Approximate line centers were estimated to be near the center of each cluster of hyperfine components; we estimate the uncertainty of these line centers to be 200 kHz. Rotational constants (Table 2) were obtained by fitting the line centers to the Watson S-reduction Hamiltonian using the I' representation;  $\Delta\nu_{\text{rms}} = (\nu_{\text{obs}} - \nu_{\text{calc}})_{\text{rms}} = 114.9$  kHz. No *c*-type transitions were observed, suggesting that the projection of the dipole moment on the *c*-inertial axis is small.

Twelve and fifteen rotational transitions were observed for <sup>15</sup>N<sub>a</sub>-prolinamide and <sup>15</sup>N<sub>2</sub>-prolinamide, respectively. Again, no *c*-type transitions could be found, despite accurate predictions based on fits of the measured transitions. The rotational transitions of <sup>15</sup>N<sub>a</sub>-prolinamide were somewhat easier to resolve due to the presence of only one quadrupole nucleus, but overlapping hyperfine structure still prevented assignment of the components. These transitions spanned approximately 300 kHz, and the estimated center frequencies have uncertainties of 75 kHz. Fits of the transitions to the Watson Hamiltonian, including the distortion constants *D*<sub>J</sub> and *D*<sub>JK</sub>, resulted in  $\Delta\nu_{\text{rms}} = 22.4$  kHz. Each rotational transition of the <sup>15</sup>N<sub>2</sub> isotopomer had only a single component with a line width of 40 kHz.  $\Delta\nu_{\text{rms}} = 3.7$  kHz for the spectral fit.

Measurements of the Stark shifts were made for five  $|M|$  components of the <sup>15</sup>N<sub>2</sub>-labeled species to avoid the complicating effects of nuclear quadrupole splittings. We measured the Stark shifts of  $M = 0$  and  $|M| = 1$  components arising from different rotational transitions because the higher  $|M|$  components had very fast Stark shifts (shifting  $\sim 500$  kHz in a 75 V/cm electric field) which could not be calibrated against OCS. The experimental Stark shifts were then fit to the *a*, *b*, and *c* components of the dipole moment by using second-order Stark coefficients calculated from the rotational constants. The best-fit values were  $\mu_a = 3.13$  (4) D,  $\mu_b = 2.21$  (2) D,  $\mu_c = 0.1$  (4) D, and  $\mu_{\text{tot}} = 3.83$  (4) D, where the large uncertainties reflect the small Stark shifts: typically  $\Delta\nu_{\text{Stark}} \leq 400$  kHz. Table 3

(18) Balle, T. J.; Flygare, W. H. *Rev. Sci. Instrum.* **1981**, *52*, 33–45.

(19) Tubergen, M. J.; Flad, J. E.; Del Bene, J. E. *J. Chem. Phys.* **1997**, *107*, 2227–2231.

(20) Tanaka, K.; Ito, H.; Harada, K.; Tanaka, T. *J. Chem. Phys.* **1984**, *80*, 5893–5905.

(21) Bodansky, M.; Bodansky, A. *The Practice of Peptide Synthesis*; Springer-Verlag: Berlin, 1994.

(22) Brieger, G.; Nestruck, T. J. *Chem. Rev.* **1974**, *74*, 567–580. Jackson, A. E.; Johnstone, R. A. W. *Synthesis* **1976**, 685–687.



**Table 3.** Comparison of the Observed and Calculated<sup>a</sup> Stark Effects for  $^{15}\text{N}_2$ -Prolinamide

transition	M	$\Delta\nu/\mathcal{L}^2$ (MHz $\text{kV}^{-2} \text{cm}^2$ )	
		obsd	calcd
3 <sub>12</sub> -2 <sub>11</sub>	0	4.0(1)	3.9
4 <sub>04</sub> -3 <sub>03</sub>	1	3.08(7)	3.21
4 <sub>14</sub> -3 <sub>13</sub>	1	5.3(3)	5.2
4 <sub>13</sub> -3 <sub>12</sub>	0	-3.20(4)	-3.28
3 <sub>03</sub> -2 <sub>12</sub>	0	-2.22(4)	-2.3

<sup>a</sup> Calculated with  $\mu_a = 3.13$  D,  $\mu_b = 2.21$  D,  $\mu_c = 0.1$  D, and the rotational constants in Table 2.

**Table 4.** Semiempirical Model Conformations

conformer	description	$\Delta I_{\text{rms}}$ , amu $\text{\AA}^2$	rel energy, kJ $\text{mol}^{-1}$
<b>1</b>	$C^\beta$ -exo/ $C^\gamma$ -endo twist	10.3	53.4
<b>2</b>	$C^\gamma$ -exo envelope	39.3	22.0
<b>3</b>	$C^\beta$ -endo envelope	41.6	56.9
<b>4</b>	amino N-endo envelope	38.8	63.3
<b>5</b>	amino N-exo envelope	44.7	165.7
<b>6</b>	planar	20.6	0.0

**Table 5.** Ab Initio Model Conformations

conformer	description	$\Delta I_{\text{rms}}$ , amu $\text{\AA}^2$	rel energy, kJ $\text{mol}^{-1}$
<b>7</b>	$C^\gamma$ -endo envelope	9.4	0.0
<b>8</b>	$C^\beta$ -endo envelope	35.9	5.2
<b>9</b>	$C^\beta$ -endo/ $C^\gamma$ -exo twist	34.1	1.2
<b>10</b>	$C^\beta$ -exo/ $C^\gamma$ -endo twist	2.1	2.4

compares the experimental Stark shifts to the shifts calculated with the best-fit dipole moment components.

## Discussion

The amide derivative of proline was chosen for these experiments because the melting point is much lower for prolinamide (95–97 °C) than for proline (228 °C). Also, proline decomposes at its melting temperature, while prolinamide is stable over a relatively large temperature range.

We used the program Hyperchem<sup>23</sup> with the AM1 parametrization to model the conformations of prolinamide starting from the default values for the bond distances and angles of the prolyl residue. Complete optimizations, in which no constraints were applied to the structure, converged to a planar ring conformation with  $\Psi = 0^\circ$  (eclipsing nitrogens about the  $\text{NC}^\gamma\text{C}^\alpha\text{N}$  dihedral angle, see Figure 1C). Other conformations, analogous to the envelope and twist structures described by Kayushina and Vainshtein,<sup>13</sup> DeTar and Luthra,<sup>14</sup> and Haasnoot et al.,<sup>15</sup> were modeled by constraining  $\Psi$  (fixed at  $0^\circ$ ) and some of the ring torsional angles; these structures are shown in Figure 2. The relative energies of the six conformers are given in Table 4, and the atomic coordinates for these structures are available as Supporting Information.

The conformations of prolinamide were also modeled at the Hartree–Fock level (6-31G\*) with PC Spartan<sup>24</sup> software (Figure 3 and Table 5). The fully optimized structure converged to a  $C^\gamma$ -endo envelope ring conformation with  $\Psi = 0^\circ$ . Two twist structures and an additional envelope conformation were found within 6 kJ  $\text{mol}^{-1}$  of the minimum energy structure. These structures may not represent local minima on the potential energy surface since  $\Psi$  and the ring torsional angles were constrained as described above. The model calculations reveal

that there are many different low-energy conformations, although the experimental spectrum may not correspond to the lowest energy structure.

The model structures were used to predict moments of inertia (using the program STRGN<sup>25</sup>) which were then compared with the experimental values for the identification of the conformation. Tables 4 and 5 report the root-mean-square averages of the differences between observed and calculated moments of inertia:  $\Delta I_{\text{rms}}$  where  $\Delta I = I_x(\text{obs}) - I_x(\text{calc})$  and  $x = a, b,$  and  $c$  for each isotopomer. The different ring conformers predict very different moments of inertia for the three isotopic species;  $\Delta I_{\text{rms}}$  ranges from 10.3 to 44.7 amu  $\text{\AA}^2$  for the semiempirical structures and from 2.1 to 35.9 amu  $\text{\AA}^2$  for the ab initio structures. In Tables 4 and 5 the  $C^\beta$ -exo/ $C^\gamma$ -endo twist conformations have the lowest  $\Delta I_{\text{rms}}$  values, although the semiempirical model is more puckered ( $\chi_{\text{max}} = 41.4^\circ$ ) than the corresponding ab initio model ( $\chi_{\text{max}} = 32.9^\circ$ ); see below. The ab initio twist conformer (**10**) has the lowest  $\Delta I_{\text{rms}}$  and therefore best describes the ring conformer observed experimentally.

The model conformations described in Tables 4 and 5 all have  $\Psi = 0^\circ$ ; the effect of this dihedral angle on the moments of inertia was systematically considered for each of the models. For conformer **10**,  $\Psi = 0^\circ$  gives  $\Delta I_{\text{rms}} = 2.1$  amu  $\text{\AA}^2$ .  $\Delta I_{\text{rms}}$  rapidly increases as the dihedral angle changes and comes to maxima at  $\Psi = 50^\circ$  and  $230^\circ$  ( $\Delta I_{\text{rms}} = 24.8$  and  $27.8$  amu  $\text{\AA}^2$ , respectively). Between these maxima, at  $\Psi = 102^\circ$ , a second region of low  $\Delta I_{\text{rms}}$  values occurs ( $\Delta I_{\text{rms}} = 2.8$  amu  $\text{\AA}^2$ ). Minima occur at different dihedral angles for the remaining conformers, but their  $\Delta I_{\text{rms}}$  values never fall below 9.0 amu  $\text{\AA}^2$ , except for conformer **1**, which has  $\Delta I_{\text{rms}} = 4.1$  amu  $\text{\AA}^2$  at  $\Psi = 80^\circ$  and  $180^\circ$ . The experimental moments of inertia eliminate all  $\Psi$  rotamers of conformers **1–9** but do not distinguish between the  $\Psi = 0^\circ$  and  $102^\circ$  rotamers of conformer **10**.

The projections of the dipole moment were used to distinguish the two rotamers of conformer **10**. Hartree–Fock calculations (6-31G\*) predict  $\mu_{\text{tot}} = 4.14$  D,  $\mu_a = -3.31$  D,  $\mu_b = 2.44$  D, and  $\mu_c = -0.48$  D for the  $\Psi = 0^\circ$  rotamer of conformer **10** and  $\mu_{\text{tot}} = 4.84$  D,  $\mu_a = -3.78$  D,  $\mu_b = 2.79$  D, and  $\mu_c = -0.57$  D for the  $\Psi = 102^\circ$  rotamer. These conformations (and all conformations **1–10**) have the amino hydrogen exo and the lone pair endo—consistent with an intramolecular hydrogen bond from the amide to the amine ( $\Psi = 0^\circ$  describes a structure with the amide oriented toward the amine). The orientation of the amide in the  $\Psi = 102^\circ$  rotamer is inconsistent with intramolecular hydrogen bonding, so the amino hydrogen may be either exo or endo. Thus another HF/6-31G\* model of conformer **10** with  $\Psi = 102^\circ$ , but with the amino hydrogen endo, was computed to have  $\mu_{\text{tot}} = 4.58$  D,  $\mu_a = -2.34$  D,  $\mu_b = 3.83$  D, and  $\mu_c = 0.90$  D. The experimental dipole components ( $\mu_{\text{tot}} = 3.83(4)$  D,  $|\mu_a| = 3.13(4)$  D,  $|\mu_b| = 2.21(2)$  D, and  $|\mu_c| = 0.1(4)$  D) are in good agreement with the dipole components predicted for the  $\Psi = 0^\circ$  conformation but are inconsistent with either prediction for the  $\Psi = 102^\circ$  conformation. The final structure of the experimental conformation is best described as a twisted ring with  $C^\beta$ -exo,  $C^\gamma$ -endo, and  $\Psi = 0^\circ$ .

The Kraitzman method<sup>26</sup> can be used to calculate the absolute values of the atomic coordinates of the nitrogens from the experimental moments of inertia (Table 6); the relative signs of the coordinates, however, must be deduced from the molecular structure. Since the center of mass is located above

(25) Schwendeman, R. H. *Critical Evaluation of Chemical and Structural Information*; Lide, D. R., Paul, M. A., Eds.; National Academy of Sciences: Washington, DC, 1974; pp 94–115.

(26) Kraitzman, J. *Am. J. Phys.* **1953**, *21*, 17–24. Gordy, W.; Cook, R. L. *Microwave Molecular Spectra*; Wiley: New York, 1984.

(23) Hyperchem, release 4; Hypercube: Waterloo, ON, 1994.

(24) PC Spartan 1.0; Wavefunction, Inc.: Irvine, CA, 1996.

**Table 6.** Nitrogen Atomic Coordinates (Angstroms) from Kraitchman Substitution Calculations

	amino nitrogen	amide nitrogen
<i>a</i>	0.874(2)	1.533(1)
<i>b</i>	0.999(2)	1.221(1)
<i>c</i>	0.628(2)	0.539(3)

$C^\alpha$  (see Figure 1), the *a* coordinates of the nitrogens have opposite signs. The relative signs of the *b* and *c* coordinates depend on the conformation and orientation of the amide; for conformer **10** with  $\Psi = 0^\circ$  the two nitrogens have the same sign for their *b* coordinates and opposite signs for their *c* coordinates. Using these Kraitchman coordinates we found that the N–N distance is 2.684(2) Å.

We used the structure of conformer model **10** to calculate the pseudorotational phase angle, *P*, and the maximum out-of-plane pucker amplitude,  $\chi_{\max}$ , using the definitions of Westhof and Sundaralingam:<sup>27</sup>  $\tan P = B/A$  and  $\chi_{\max} = (A^2 + B^2)^{1/2}$ . The torsional angles and origin of the pseudorotational cycle were defined according to Schmidt et al.,<sup>28</sup> the constants *A* and *B* can then be calculated by using

$$A = \frac{2}{5} \sum_{i=0}^4 \chi_i \cos\left(\frac{4\pi}{5}(i-2)\right)$$

and

$$B = -\frac{2}{5} \sum_{i=0}^4 \chi_i \sin\left(\frac{4\pi}{5}(i-2)\right)$$

Structure **10** has  $P = 185^\circ$  and  $\chi_{\max} = 32.9^\circ$  and is consistent with the conformations determined from NMR and X-ray crystallography; structure **10** is especially close to the S-domain conformation of prolinamide derived from NMR coupling constants ( $P_S = 192^\circ$  and  $\chi_{\max,S} = 33.3^\circ$ ).<sup>15</sup> In the analysis of the prolinamide NMR data, the  $^3J_{\text{HH}}$  NMR coupling constants

(27) Westhof, E.; Sundaralingam, M. *J. Am. Chem. Soc.* **1983**, *105*, 970–976.

(28) Schmidt, J. M.; Brüschweiler, R.; Ernst, R. R.; Dunbrack, R. L.; Joseph, D.; Karplus, M. *J. Am. Chem. Soc.* **1993**, *115*, 8747–8756.

were simultaneously fit to the pseudorotational parameters for both N- and S-domain conformations and the relative amounts of the two conformations, described by the mole fraction of the N-domain conformation. The corresponding N-domain parameters from solution NMR ( $P_N = -3.0^\circ$  and  $\chi_{\max,N} = 38.2^\circ$ ) are very similar to model structure **9** ( $P = -3.6^\circ$  and  $\chi_{\max} = 39.3^\circ$ ) and describe a twist structure with  $C^\beta$ -endo and  $C^\gamma$ -exo. Since the mole fraction fit to 0.5, both conformations are equally populated in solution. Structure **9** is inconsistent with the experimental microwave spectra because of its large  $\Delta I_{\text{rms}}$  value. While no spectroscopic evidence (such as unassigned transitions) for a second conformation was observed in the 875 MHz frequency range searched, we cannot eliminate the possibility of additional stable conformations in the expansion.

## Conclusions

Experimental moments of inertia of three isotopomers of prolinamide were compared to several semiempirical and ab initio models. A twist  $C^\beta$ -exo/ $C^\gamma$ -endo structure reproduces the experimental values best. Stark effect measurements were used to find  $\mu_{\text{tot}} = 3.83(4)$  D; both dipole moment and moment-of-inertia data were used to determine that the  $\text{NC}^\beta\text{C}^\alpha\text{N}$  dihedral angle is approximately zero. The Kraitchman analysis of the experimental moments of inertia indicates that the N–N distance is 2.684(2) Å for this conformation.

**Acknowledgment.** This work was supported by a grant from the National Science Foundation (CHE-9700833). Acknowledgment is also made to the donors of the Petroleum Research Fund, administered by the American Chemical Society, for the support of this research. The authors wish to thank Dr. Thomas Janini, Dr. James Dudones, and Professor Paul Sampson for helpful discussions regarding the synthesis of the isotopically labeled species.

**Supporting Information Available:** Tables of principal axis atomic coordinates of model conformations **1–10** (10 pages print/PDF). See any current masthead page for ordering information and Web access instructions.

JA981775Z